Neuron, Vol. 18, 959–968, June, 1997, Copyright ©1997 by Cell Press

The Efficiency of Sensory Information Coding by Mechanoreceptor Neurons

Mikko Juusola* and Andrew S. French
Department of Physiology and Biophysics
Dalhousie University
Halifax, Nova Scotia B3H 4H7
Canada

Summary

Most sensory systems encode external signals into action potentials for transmission to the central nervous system, but little is known about the cost or efficiency of this encoding. We measured the information capacity at three stages of encoding in the neurons of a spider slit-sense mechanoreceptor organ. For the receptor current under voltage clamp, the capacity was ~1400 bits/s, but when the neuron was allowed to generate a receptor potential, nonlinear membrane processes improved the capacity to >2000 bits/s. Finally, when action potentials were produced, the capacity dropped to ~200 bits/s, or ~14% of the receptor current capacity. These measurements provide a quantitative estimation of the cost of encoding analog signals into action potentials.

Introduction

Mechanoreceptor neurons usually transform a continuously varying mechanical stimulus into trains of discrete action potentials. This transformation has traditionally been viewed as a three-stage process. First, the input stimulus modulates the opening of mechanically sensitive ion channels, generating a transmembrane ion flux called the receptor current. Second, the receptor current passing through other membrane conductances creates a voltage across the membrane, the receptor potential. Third, the receptor potential is encoded into action potentials by voltage-sensitive ion channels (Sachs, 1986; Morris, 1990; French, 1992). Each of these stages may be expected to add noise and filter the transmitted signal. While the general properties of this cascade have been understood for many years, technical difficulties and a lack of suitable preparations have so far prevented simultaneous observation of each stage in the same cell.

Sensory systems operate to optimize early neural processing, so that sufficient information about the stimulus can be reliably transmitted to the CNS via the subsequent noisy channels (van Hateren, 1992; Juusola et al., 1995, 1996). One general strategy in such coding schemes is to obtain a high signal-to-noise ratio in the responses that drive action potential production (Laughlin, 1987; Juusola et al., 1995; de Ruyter van Steveninck and Laughlin, 1996). To accomplish this, the first two stages of signal processing, the receptor current and potential, should be tuned to enhance important stimulus frequencies and to limit the effects of noise. For the mechanoreceptor neurons used in the present study, we have already shown that the earliest stages of the transduction machinery adapt to constant mechanical stimuli (Juusola and French, 1995b), allowing a high dynamic sensitivity to be used over a range of mean stimulus levels.

The mechanoreceptor preparation used here is a spider slit-sense organ that allows electrophysiological study at each stage of sensory signal encoding (Juusola et al., 1994; Juusola and French, 1995a, 1995b). The cuticle of the spider, *Cupiennius salei*, has a large number of slit-sense organs, which respond to forces causing strain in the cuticle (Barth, 1985). The anterior lyriform organ VS-3 (nomenclature of Barth and Libera, 1970) is located on the anterior-ventral side of the leg patella. It has seven to eight cuticular slits, ranging from 15–120 μm in length, each innervated by a pair of spindle-shaped bipolar neurons, which transduce strain-induced slit displacements into action potentials to be carried to the central nervous system. The animal's behavior and the locations of the slit-sense organs, e.g., on the anterior-ventral surface on the patella, suggest that the biologically relevant information is the dynamic strain, which can reflect stepping patterns, substrate vibrations, and muscular forces (Barth, 1985).

In the present study, we were able separately to observe the dynamics of the receptor current, receptor potential, and action potentials in the same mechanoreceptor neuron during dynamic mechanical stimulation. Repeated presentations of the same long sequence of Gaussian pseudorandomly modulated displacement stimuli allowed us to measure the information capacity separately at each of the three stages of sensory encoding. While our results give a good indication of the costs and efficiencies involved in these processes, they also imply that a simple cascade model is inadequate for a quantitative understanding of mechanotransduction.

Results

Receptor Current, Receptor Potential, and Action Potential Responses to the Same Stimuli

Recent advances in recording techniques with spider slit-sense organs (Figure 1) have made it possible to record the receptor current, receptor potential, and action potential responses in the neurons while mechanically displacing the slits of the organ (Juusola et al., 1994; Juusola and French, 1995a, 1995b; Figure 2). Each slit is innervated by two types of mechanosensory neurons. "Multiple-spike" neurons respond to step displacements by producing an adapting burst of action potentials, while "single-spike" neurons fire only one action potential (Juusola and French, 1995b). Because of their more vigorous responses, only multiple-spike neurons were studied here. Action potentials (AP; 50–80 mV) superimposed on receptor potential were recorded with intracellular electrodes during mechanical stimulation. Following treatment with tetrodotoxin (TTX) to

*Current address: Physiological Laboratory, University of Cambridge, Downing Street, Cambridge CB2 3EG, UK.

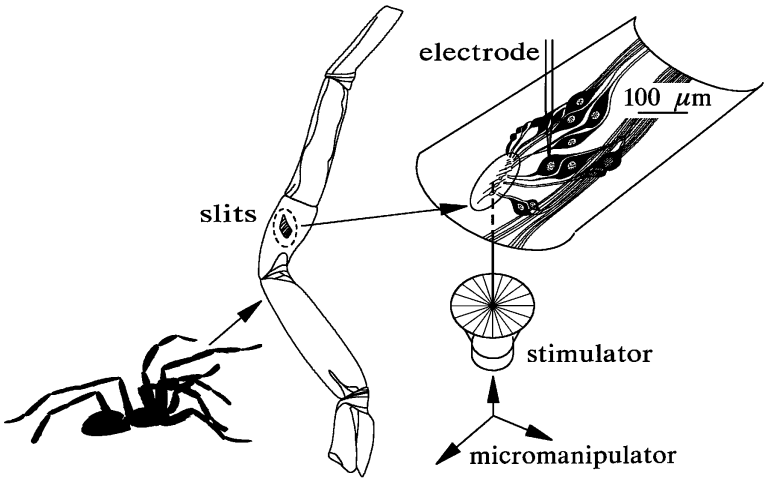

Figure 1. The Spider Slit-Sense Organ and the Stimulation Arrangement

A piece of patellar cuticle containing the anterior lyriform slit-sense organ with neurons was waxed to a custom-designed bath. A microelectrode penetrated the neurons from above, while mechanical stimulation was applied to the dry exterior of the slits from below.

block action potentials, receptor currents (RC; maxima: 0.5–1.3 nA) and receptor potentials (RP; maxima: 12–25 mV) were recorded in the same cell using identical stimuli (Figures 2A and 2B). All the cells studied showed similar response characteristics during dynamic stimulation.

Receptor Current, Receptor Potential, and Action Potential Frequency Responses

The use of a pseudorandom Gaussian stimulus allows rapid measurement of system performance over a wide frequency bandwidth (Marmarelis and Marmarelis, 1978) and has the additional advantage of resembling natural

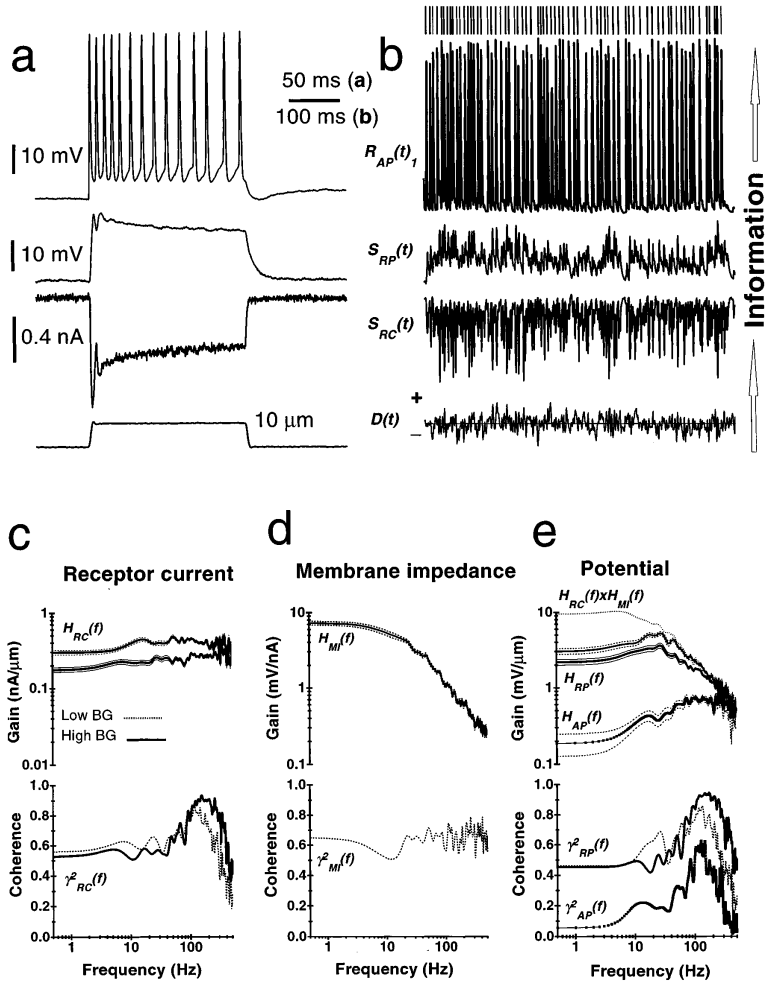

Figure 2. Typical Mechanoreceptor Responses to Displacement Stimuli

(A) Step displacements (lowest trace) produced an adapting burst of action potentials superimposed on the receptor potential. TTX-treatment blocked the action potentials, revealing the receptor potential (second trace, current clamp) and the receptor current (third trace, voltage clamp).

(B) The same traces as in (A), but using a pseudorandomly modulated displacement stimulus, $D(t)$, repeated ten times. The action potential response, $R_{AP}(t)$, is from a single sweep, but the receptor current, $S_{RC}(t)$, and receptor potential, $S_{RP}(t)$, were averaged ten times. Receptor current, receptor potential, and action potential responses were recorded during 10–30 presentations of an 8.192 s sequence of pseudorandomly modulated stimulus, using two different mean displacement levels with the same modulation depth (low, 5 ± 2 mm, and high, 10 ± 2 mm, $\mu \pm \sigma$). Responses to repeated pseudorandom sequences were averaged to obtain the noise-free signals, $S_{RC}(t)$, $_{SRP}(t)$, and SAP(t), that were used in calculating the corresponding frequency response functions.

(C–E) Above, the receptor current, receptor potential, and action potential frequency response functions, $H_{RC}(f)$, $H_{RP}(f)$, and $H_{AP}(f)$, respectively, and the membrane impedance function, $H_{MI}(f)$, with corresponding 95% confidence intervals. Below, the corresponding coherence functions, $\gamma^2_{RC}(f)$, $\gamma^2_{RP}(f)$, $\gamma^2_{AP}(f)$, and $\gamma^2_{MI}(f)$. Results for high and low background displacements (BG) are shown as solid and dashed lines, respectively.

strain modulation of the spider exoskeleton (Bohnenberger, 1981). After repeated presentations of the same displacement stimulus (Figure 2B), frequency response functions, $H_X(f)$, and coherence functions, $\gamma^2_X(f)$, were calculated for each stage of sensory processing, using the corresponding averaged responses as the output signal and the displacement stimulus as the input signal (Bendat and Piersol, 1971; Marmarelis and Marmarelis, 1978; Figures 2C–2E). The coherence function, $\gamma^2(f)$, provides a normalized measure of the linear correlation between two signals as a function of frequency, f (Bendat and Piersol, 1971). Confidence intervals (95%) for the gains of the frequency response functions were calculated from the coherence functions (French et al., 1972). We have shown earlier that responses in these neurons adapt rapidly and nonlinearly to different mean background displacements and maintain their high sensitivity over a wide range (within 10–20 μm; Juusola and French, 1995b). Here, we measured the responses at two different background displacement levels of 5 μm and 10 μm (low BG and high BG), which depolarized the neurons by ~7 mV and ~10 mV, respectively. After ~30 s adaptation, the responses stabilized and the recordings at the two levels were highly reproducible.

Based on the coherence function, mechanotransduction to the receptor current operated linearly at relatively high frequencies (60–400 Hz), where $\gamma^2_{RC}(f) \approx 0.7$ (Figure 2C) before falling as the output of the stimulator declined to zero. The form of the frequency response function between input displacement and receptor current, $H_{RC}(f)$, was similar at different background displacements, with a monotonic increase in gain from 0.5–400 Hz that was well approximated by a linear fit (cf. Juusola and French, 1995b). Similar behavior has been reported before in a variety of mechanoreceptors (French, 1992). The lower coherence at low frequencies reflects the nonlinear change in gain that accompanies adaptation to different mean background displacements (Juusola and French, 1995b).

For the receptor potential, $H_{RP}(f)$, the peak signal amplitude occurred at mid-range frequencies (10–100 Hz), indicating that the cell membrane low-pass filters the receptor current signal (Figure 2E). This was confirmed during static displacement (low BG) by injecting pseudorandomly modulated current (±1 nA RMS) through the recording electrode to calculate the membrane impedance, $H_{MI}(f)$, directly, i.e., between the injected current stimulus and the resulting voltage response. Multiplying $H_{MI}(f)$ by $H_{RC}(f)$ gave a good approximation to $H_{RP}(f)$ at stimulus frequencies above 10 Hz (Figure 2E), confirming this hypothesis. However, below 10 Hz there was substantial nonlinearity in both the membrane impedance and the transduction current, as seen in the low values of the corresponding coherence functions. This could explain the discrepancy between the estimated and recorded receptor potential frequency responses at low frequencies.

The frequency response function between the displacement stimulus and action potentials, $H_{AP}(f)$, showed high-pass characteristics (Figure 2E), responding most vigorously above 80 Hz. The coherence for action potential production, $\gamma^2(f)$, was much lower than for the analog signals but, again, peaked at relatively high frequencies.

Defining Signal and Noise

Repeated presentations of identical pseudorandom signals allowed measurement of the noise-free response to be obtained by averaging (cf. Juusola et al., 1995). Subtraction of the average response then gave the noise component of each individual response.

For the analog receptor current and receptor potential, the encoded signal was obtained from the average response to multiple presentations of an identical stimulus, while the noise was estimated from the differences between individual responses and the average response (Figures 3A and 3B; see Experimental Procedures: Signal Analysis in the Time Domain). To test if the dynamic stimulus would affect the intrinsic noise level of the neurons, we also recorded the noise level in the same neurons during a static displacement stimulus of the same mean value.

For action potentials, the signal, $S_{AP}(t)$, was defined as the probability of an action potential falling within each 1 ms period, obtained from the total action potentials in each period divided by the number of stimulus presentations (Figure 3C). This method of counting action potentials into narrow time bins is equivalent to the method used previously for obtaining regularly sampled values from stochastic trains of action potentials (Sakuranaga et al., 1987), and is also equivalent to the French-Holden Algorithm (French and Holden, 1971) for optimal alias-free sampling of action potentials, if the action potentials are assumed to occur at the center of each sampling period (see Experimental Procedures). Action potential duration is ~1 ms in these neurons (Seyfarth and French, 1994), and postsynaptic responses to action potentials may be longer. In addition, the receptor potential signal and noise amplitudes in the experiments were negligible below 500 Hz (Figure 3E). Therefore, a bin width of 1 ms was appropriate for recording the action potentials. Noise in the action potential signal, $N_{AP}(t)$, was measured from the differences between the action potential counts in individual response periods and the mean counts from all of the presentations (Figure 3C).

Characteristics of the Signal and Noise Data

Dynamic displacement stimulation elicited receptor current responses, $R_{RC}(t)_i$, that were highly reproducible and had noise values, $N_{RC}(t)_i$, much smaller than the signal, $S_{RC}(t)$ (Figure 3A). Since the neurons were voltage clamped to −5 to −10 mV below the resting potential, the receptor current noise during the displacement stimuli must have been almost entirely due to the mechanotransduction channels, because the activation of voltage-sensitive channels is not significant below the resting potential (see Experimental Procedures). Similarly, the receptor potential responses, $R_{RP}(t)_i$, to dynamic displacement stimulation were also highly reproducible, and the corresponding noise values, $N_{RP}(t)_i$, were even smaller than those measured under voltage clamp (Figures 3A and 3B). The action potential responses to the same stimuli displayed highly repeatable spiking patterns; but, at the level of single histogram bins, there was relatively larger variance than seen with the preceding analog responses (Figure 3C).

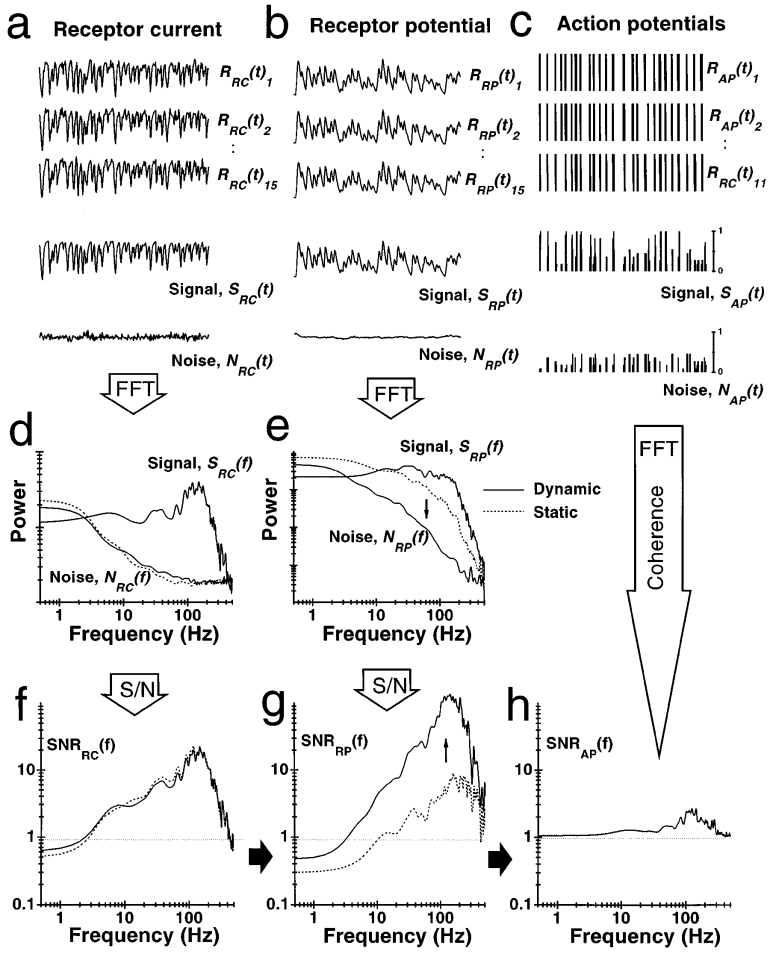

Figure 3. Measuring Signal-to-Noise Ratios

Calculation of $SNR_X(f)$ (A–C); 300 ms traces of receptor current, $R_{RC(t)}$, receptor potential, $R_{RP}(t)$, and the probability of action potential firing, $R_{AP}(t)$, and their corresponding noise estimates, $N_x(t)_i$, from a single stimulus run (lower traces). After frequency domain averaging the receptor current and potential signals and all noise data (D and E), the signal-to-noise ratios of the analog processing were calculated using Equation 1 (F and G). For action potentials, the $SNR_{AP}(f)$ was calculated from the corresponding coherence function (H).

Characteristics of the Signal and Noise Spectra

The static and dynamic noise data, $S_x(t)$ and $N_x(t)_{is}$, $N_x(t)_{id}$, were Fourier transformed to give signal and noise power spectra, $S_{xx}(f)$ and $N_{xx}(f)_s$, $N_{xx}(f)_d$. The action potential responses were not subjected to this analysis. Instead, their responses and coherence functions were used directly for estimating the performance of action potential encoding in terms of signal-to-noise ratio and information capacity, as described below.

For the receptor current, the noise spectra during dynamic displacement stimuli at the same mean displacement level did not vary significantly from the static condition (Figure 3D, continuous line), indicating that dynamic operation of the mechanotransduction channels did not produce much additional noise (this estimation also included the noise generated by the voltage clamp circuitry; see Experimental Procedures). However, the situation was very different for the receptor potential. Here, static mean displacement depolarized the neurons to 5–15 mV above the resting potential, where the noise spectrum was influenced by the activities of both mechanotransduction channels and several classes of voltage- and calcium-sensitive channels, which do not inactivate at these potentials (see Experimental Procedures; Figure 3E, dashed line). With dynamic stimulation, the noise level in the neurons decreased dramatically, suggesting that interactions between the various ion channels and the membrane capacitance produce significant nonlinear filtering and improvement of the signal-to-noise ratio.

Signal-to-Noise Ratios at the Three Stages of Sensory Encoding

For the receptor current and potential, $SNR_{RC}(f)$ and $SNR_{RP}(f)$ were calculated as functions of frequency (Figures 3D–3G):

$$SNR_x(f) = S_{xx}(f)/N_{xx}f \quad (1)$$

For action potential encoding, $SNR_{AP}(f)$ was calculated from the corresponding coherence function (Bendat and Piersol, 1971):

$$SNR_{AP}(f) = 1/(1 - \gamma^2_{AP}(f)) - 1 \quad (2)$$

The efficiency of transduction, as measured by receptor current $SNR_{RC}(f)$, was independent of the noise spectra used and high over most of the tested frequency range, peaking at 150–200 Hz with SNR ≈ 30 (Figure 3F). The corresponding SNR for the receptor potential, $SNR_{RP}(f)$, depended on the noise spectra used in the calculations. With static displacement, the SNR for receptor potential was lower than for receptor current, but with dynamic stimulation, $SNR_{RP}(f)$ was similar to $SNR_{RC}(f)$ at low frequencies and improved ~10-fold compared with current

at high frequencies, peaking at 150–200 Hz with SNR = 100–300 (Figure 3G). Finally, action potential encoding reduced the measured SNR values significantly, as expected. However, $SNR_{AP}(f)$ still exceeded unity over the 100–200 Hz region (Figure 3H).

As suggested above, the most reasonable explanation for the higher SNR in the dynamically stimulated receptor potential is that the unclamped membrane potential allows nonlinear interactions between the various types of ion channels in the membrane, which are impossible under voltage clamp, with the greatest improvement being caused by removal of high frequency noise (Figure 3E). Dynamic displacement stimulation induces a correspondingly dynamically changing membrane potential that causes interactions between the various membrane conductances, improving the SNR. During static displacements, which lack the interaction between the dynamic transduction current and voltage- and calcium-sensitive conductances (see Experimental Procedures), this nonlinear, frequency selective noise reduction must be much less effective.

Information Capacity at the Three Stages of Sensory Encoding

Information capacity is the maximum achievable rate of information transmission through a communication system in bits per second, using the optimum signal encoding (Shannon, 1949). The use of Gaussian stimulation in the experiments and the observed signal and noise properties (see Experimental Procedures: Properties of the Signal and Noise Estimates) allowed us to calculate the information capacity from each measured set of signal-to-noise ratios (Figures 3D–3G) using the Shannon formula (1949):

$$R_{info} = \int \log_2(1 + SNR_x(f))\, df \qquad (3)$$

Because of the difference between the action potential signals and the analog signals, we used two different methods, coherence function and maximum entropy, to calculate the information capacity for the production of action potentials (see Experimental Procedures). These methods each gave slightly different estimates of the information capacity at the final encoding stage.

Nonlinear filtering by the cell membrane caused the efficiency of transduction to be higher under current clamp than under voltage clamp, increasing the information capacity from 1430 ± 210 bits/s to 2240 ± 480 bits/s ($\mu \pm \sigma$, n = 5; Figure 4). This seems important because the efficiency of action potential encoding was only about 9% of the receptor potential efficiency (200 ± 40 bits/s; $\mu \pm \sigma$, n = 5), so that the overall information capacity in the action potential signal was about 13–15% efficient. Although this value is low, the neurons generated highly repeatable action potential responses with a 10–20% noise level.

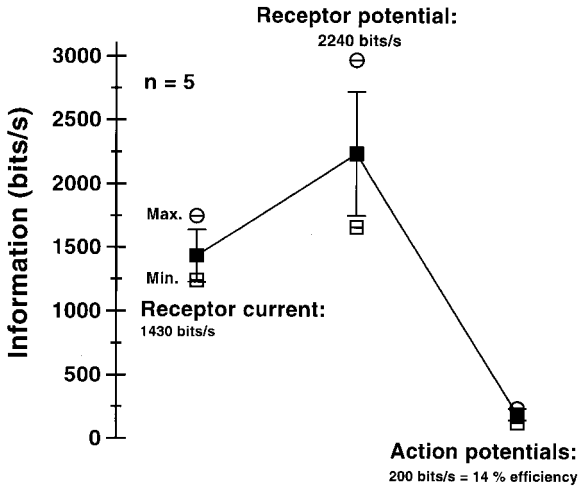

Figure 4. Information Capacities at Each Stage of Mechanotransduction

Information capacities for the receptor current and receptor potential were calculated from signal-to-noise ratios, $SNR_{xx}(f)$, using the Shannon Equation 3. All data are shown as mean and standard deviations from five experiments. This figure shows the results calculated from the coherence method. Mean values for the three stages were significantly different from each other, using a t test ($P < 0.05$).

Discussion

Our findings show that action potential encoding occurs relatively inefficiently in spider slit-sense organ mechanoreceptor neurons. The information capacity in the analog receptor current and receptor potential signals in these multiple-spike neurons was comparable to the maximum estimated information transmission rates for analog signals in blowfly photoreceptors and interneurons (de Ruyter van Steveninck and Laughlin, 1996). Similarly, the information capacities of the action potential signals were comparable to the maximum estimated information transmission rates for action potential encoding in fly movement detection neurons (de Ruyter van Steveninck and Bialek, 1988), in cricket cercal afferents (Levin and Miller, 1996; Roddey and Jacobs, 1996; 75–200 bits/s), in bullfrog sacculi (Bialek et al., 1991), and in electric fish (Gabbiani et al., 1996; Wessel et al., 1996). Information is lost when graded signals are converted into action potentials (Stemmler, 1996), but the situation here agrees with recent reports for action potential encoding in the catfish retina (Sakai and Naka, 1995) and in rat hippocampal neurons (Mainen and Sejnovski, 1995), which indicate that neurons can accurately convert dynamic transient signals into action potentials. While the receptor potential cannot be viewed in isolation from the action potentials, it seems likely that in these spider neurons, a high signal-to-noise ratio is achieved in the receptor potential by removing high frequency intrinsic noise in the receptor current. The production of action potentials for distance transmission comes at an overall cost of ~86% loss of information capacity.

Increased Information Transfer from Receptor Current to Receptor Potential

One of the most interesting findings of this study was the improved SNR from receptor current to receptor potential during the dynamic displacement stimulus. This robust phenomenon, which was seen in every recording series, cannot be easily explained by the simple

cascade model of mechanotransduction. This would require that the combination of the first and second stages of the cascade has a higher information capacity than the first stage alone. The explanation for this apparent paradox is probably that signal encoding by mechanoreceptors can not be modeled as a simple cascade. Instead, mechanically activated channels act in parallel with voltage- and calcium-gated channels, so that their conductances interact with each other in charging and discharging the membrane capacitance. Therefore, the receptor currents occurring under voltage clamp and current clamp conditions are not identical, nor are they the same as would occur when action potentials are firing. We must interpret our results as indicating what the SNR would be if the neuron only used current as a signal, or if it only used a passive impedance to convert the receptor current to receptor potential.

Limitations of the Methods

The information capacities measured here represent maximum achievable rates with optimum coding, rather than the actual rates occurring during our experiments. Maximum rates can be achieved with white Gaussian signals, but we do not know what the natural signals would be in this system. Information capacity cannot be calculated explicitly for systems with arbitrary noise, but limits can be calculated by assuming that the signal has finite bandwidth and limited mean power (Shannon and Weaver, 1949; Schwartz, 1963). In this case, it is also necessary to include the effects of nonwhite noise by calculating the total entropy power of the noise (Equations 9 and 10). Applying this calculation to the data of Figures 3D–3E as an example gave ranges of 1,451–1,457 bits/s for the receptor current and 3,243–3,287 bits/s for the receptor potential. These values suggest that Equation 3 gives conservative estimates of the information capacities, and that the increased information capacity in the receptor potential is not an artefact of the different noise spectra in the two measurements.

It is important to realize that no currently available technology can really observe each stage of mechanotransduction simultaneously under natural conditions. The receptor current under voltage clamp cannot be identical to that during current clamp (cf. Robinson and Kawai, 1993), and neither the receptor current nor the receptor potential can be the same when action potentials are firing. Under each of these three conditions, but particularly the latter two, complex nonlinear interactions occur between the various ion channels in the cell membrane and the membrane capacitance. Therefore, a complete quantitative demonstration of this nonlinear interaction between various conductances would require detailed knowledge of all of the ionic conductances and the other current-generating processes present in the neuron, as well as their location, and the accurate morphology of the neuron, to allow some picture of the spatial distributions of the various currents and voltages. Because of our limited knowledge of these processes, such complete modeling cannot yet be attempted. Nevertheless, the present results give a good estimate of information capacity at each stage in these sensory neurons, and show that there is a large loss of information capacity during action potential encoding.

Experimental Procedures

Animals and Preparation

Adult female (>1 year old) tropical hunting spiders (*Cupiennius salei*) Keys. (ctenidae) from a laboratory colony were used in the experiments. The spiders were maintained in plastic jars under controlled humidity at room temperature (~21°C) and were fed with Drosophila and cockroaches. A leg was autotomized, and a concave piece of cuticle containing lyriform slit-sense organ VS-3 was dissected from the anterior patella and prepared for recording under a dissecting microscope. More detailed descriptions of this initial procedure are given by Seyfarth and French (1994).

The piece of cuticle containing the slit-sense organ was attached with beeswax to a custom-designed preparation holder that functioned as a bath, filled with spider saline (442 mOsm: 223.0 mM NaCl, 6.8 mM KCl, 8.0 mM $CaCl_2$, 5.1 mM $MgCl_2$, and 11 mM sucrose [pH 8.2]; Maier and Seyfarth, 1987) and grounded with an indifferent electrode (Ag/AgCl) positioned close to the sensory neurons. The bath was equipped with a hose-system that allowed solution changes for chemical treatment or adjustment of the saline level, when necessary. Diffusion of oxygen from the air was sufficient to maintain the electrical properties of the neurons, even with experiments lasting several hours. The details of the preparation are found in Juusola and French (1995a, 1995b).

Microelectrodes

The microelectrodes were pulled with a horizontal laser puller (P-2000, Sutter Instrument Company, USA) from filamented borosilicate glass capillaries (Hilgenberg, Germany), with inner and outer diameters of 0.5 mm and 1.0 mm, respectively. The electrodes were backfilled with the electrolyte (3M KCl) and coated with Dricote (Fisher) and Vaseline. The resistance of the microelectrodes inside a cell varied between 30 and 70 MΩ. The time constant of the electrodes, τ_e, in tissue after a dual capacitance compensation of the amplifier (SEC-1L, npi electronic, Germany) was 2–3 μs, giving a high cutoff frequency of ~60 kHz. The advantages and use of the coated microelectrodes in voltage clamping the spider slit-sense organ mechanoreceptor neurons are explained in Juusola et al. (1997).

Mechanical Stimulation

All of the experiments were done using a closed-loop mechanical stimulator (Chubbuck, 1966), which was mounted firmly below the preparation holder. Computer-aided stimulation of the mechanoreceptor neurons was performed using steps or pseudorandomly modulated displacements directed to the exterior face of the slit-sense organ from below by a stiff, plastic, needle-shaped probe (Juusola and French, 1995a, 1995b). The stimulator was driven by an independent current source, whose output was second-order compensated. The stimulus range, measured by displacement of the stimulus probe, was up to 20 μm with 0.05 μm resolution. At the start of each experiment, the zero displacement level was established by raising the probe under computer control until it contacted the surface of the slit-sense organ cuticle. This was detected by action potential production. Next, the probe was lowered so that no stimulus-induced neural activity could be detected. The tip of the stimulus probe could be seen under illumination through the transparent cuticle and its location could be controlled by a three-dimensional micromanipulator.

The pseudorandom displacement output of the stimulator was Gaussian and had significant power from 0–300 Hz, above which it gradually declined (Figures 5A and 5B, continuous lines). Some early experiments were done with another closed-loop stimulator, based on a small loudspeaker (cf. Juusola and French, 1995a, 1995b). This stimulator had a wider output bandwidth, with an approximately flat spectrum up to 400 Hz, but had worse resolution and resonance compensation than the other stimulator (Figure 5B, dotted line; Juusola and French, 1995b). However, when driven with pseudorandom

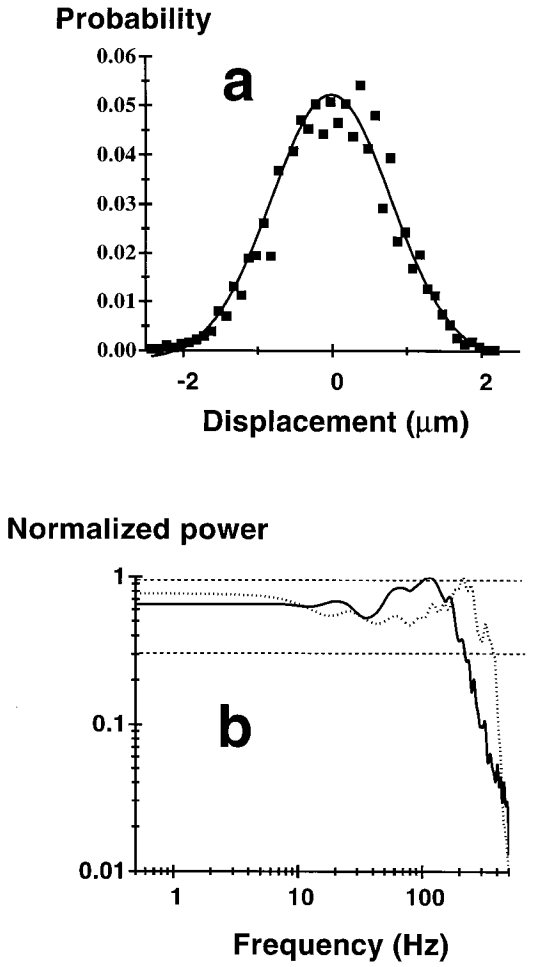

Figure 5. Properties of the Pseudorandomly Modulated Displacement Stimuli

(A) Probability density function of the stimulator output was Gaussian.

(B) The flat power spectra of the output (i.e., displacement stimuli) of the two stimulators used in this study. The continuous line represents the Chubbuck-stimulator; the dotted line is the loudspeaker based stimulator (see Experimental Procedures).

modulation, both stimulators produced receptor current frequency responses of similar shape and bandwidth (cf. Figure 2B in this paper and Figure 8 in Juusola and French, 1995b). As the receptor current responses had the highest bandwidth, the other neural frequency response, coherence, and SNR functions (see below) of the spider mechanoreceptor neurons were reliably measured within the frequency range from 0.5–350 Hz.

It should be stressed that the present results are based on stimuli with finite bandwidth, and only reflect the system's information capacities under these particular conditions. For example, the stimulators were not able to generate sufficiently high frequencies to fully match the fast time course of the receptor current transients (cf. Juusola and French, 1995b). Hence, the shape of receptor current power spectra at high frequencies (>300 Hz) at least partially reflect the limited bandwidth of the stimulators. Together with the smooth high frequency noise spectra of the receptor current, it is likely that the limited bandwidth reduced the high frequency $SNR_{RC}(f)$ and information capacity of the receptor current. However, this bias was at least partially compensated by the natural skew of the receptor current signal (see below: Properties of the Signal and Noise Estimates).

The stimulator and the entire experimental arrangement were mounted on a gas-driven vibration isolation table (Technical Manufacturing, Micro-g), and all of the experiments were performed at room temperature (22°C ± 2°C).

Recording Procedures During Pseudorandom Gaussian Stimuli

This study was based on five preparations in which recordings from single multiple-spike neurons were stable for several hours, allowing complete series of receptor current, receptor potential, and action potential recordings. The neurons were adapted for 30 s to the mean displacement before starting the dynamic stimulus modulation. This adaptation period was sufficient to complete the adaptational decay of the receptor current and to ensure that the sensitivity of the neurons had reached a steady level (Juusola and French, 1995b). For each dynamic stimulation session, a new pseudorandom stimulus sequence was obtained from a computer shift-register generator and used throughout the recordings (i.e., for evoking action potentials, receptor potential, and receptor current; see below). The recordings were done intracellularly, using an 8.192 s pseudorandomly modulated slit displacement stimulus, which was repeated 10–30 times for each experiment. Action potential responses were recorded first, and were stored with the corresponding stimulus presentations on a hard disk, to be analyzed off-line. Next, 10 μM tetrodotoxin (TTX) was added to the bath. TTX abolished the major inward currents due to blockade of voltage-sensitive sodium channels, and thus eliminated the generation of action potentials. The TTX effect was complete in about 5–10 min, after which we first recorded the corresponding receptor current responses under discontinuous single-electrode voltage clamp (dSEVC), and the corresponding receptor potential responses under discontinuous single-electrode current clamp (dSECC), to the same stimulus sequence. Some experiments were repeated using different pseudorandom stimulus sequences on the same preparation. Different stimulus sequences had no obvious effects on the calculated signal and noise power spectra (see below).

The receptor current, receptor potential, or action potential responses were transmitted via a microelectrode to a high impedance preamplifier (SEC-10L, npi electronic, Germany; 1L headstage) and filtered at 600–2400 Hz (SEC-10L; four-pole Bessel filter). With dSEVC, the stability of the voltage clamp was ensured by continuously monitoring the headstage potential. To be sure that the receptor current signal was not contaminated by various other membrane conductances, the membrane potential was held at 5–10 mV below the activation threshold (∼−75 mV) of the voltage-gated conductances (Juusola and French, unpublished data). In the dSEVC mode, the electrode current was controlled by a negative feedback amplifier. Comparing many cell responses in both dSEVC and dSECC modes, we estimated that the noise induced by the voltage clamp circuit constituted ∼20% of the total noise seen in receptor current recordings. Therefore, this noise alone could not explain why $SNR_{RC}(f)$ was lower than $SNR_{RP}(f)$. However, the $SNR_{RC}(f)$ estimates should be viewed as the lower limits of the actual $SNR_{RC}(f)$ values (cf. Figures 3C and 3E; see below).

The paired input (displacement) and output (receptor current, receptor potential, or action potential) were sampled at more than twice the signal bandwidth (1000–2500 Hz), digitized with a 12-bit A/D converter (DT2821, Data Translation, USA), and stored on a computer (IBM compatible) hard disk or on a video tape. The sampling process was initiated synchronously to the stimulus modulation produced by the computer, and 8.192 s records of both signals were obtained during each recording cycle. After a preset number of responses, the average response was calculated. The data processing was performed using ASYST 4.0 (Keithley, USA) based programs (Juusola, 1994; Juusola and French, 1995b), using conventional techniques (Bendat and Piersol, 1971; Marmarelis and Marmarelis, 1978).

Signal Analysis in the Time Domain

The respective signals, $S_x(t)$, were obtained by averaging the receptor current, $R_{RC}(t)$, the receptor potential, $R_{RP}(t)$ and the action potential, $R_{AP}(t)$, responses from repeated presentations of the same

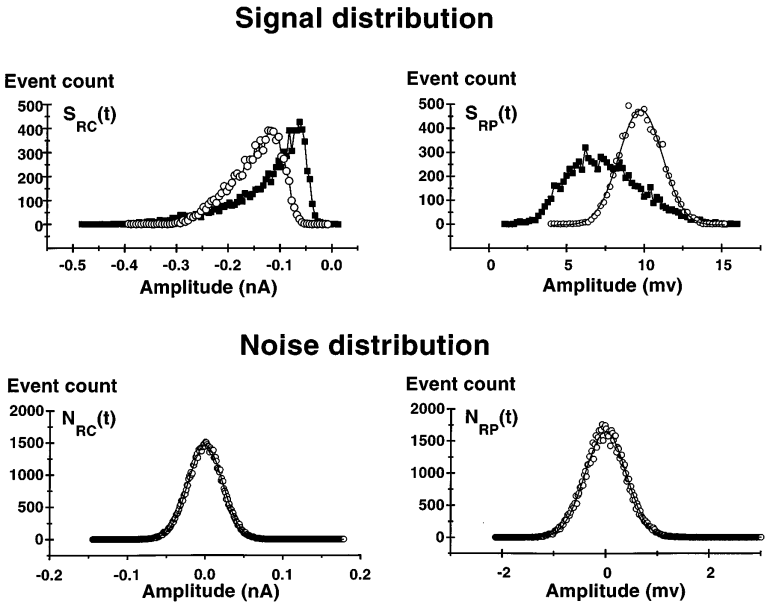

Figure 6. Signal (Upper) and Noise (Lower) Distributions of Receptor Current and Potential

The $S_{RC}(t)$ distribution was skewed at both higher (open symbols) and lower (solid symbols) mean displacement levels (cf. Juusola and French, 1995b), but at higher mean displacement the $S_{RP}(t)$ distribution was approximately Gaussian. The noise superimposed on the graded mechanoreceptor signals had a Gaussian distribution, regardless of the mean displacement.

pseudorandom displacement. To avoid possible bias of the noise estimates by the relatively small number of samples, we recalculated the noise using a method that did not allow signal and noise to be correlated, but additive. For example, when an experiment consisted of ten trials, nine of the trials were used to compute the mean and the other to compute the noise. This was repeated for each possible set of nine responses, giving ten noncorrelated noise traces. We also calculated the corresponding noise estimates by simply subtracting each $S_x(t)$ from the individual responses, $R_x(t)_i$, to yield $N_x(t)_i = R_x(t)_i - S_x(t)$. These two methods gave similar noise estimates with very low variance. Errors due to residual noise in $S_x(t)$ were small and proportional to noise power/$\sqrt{n}$ (Kouvalainen et al., 1994).

For action potentials, the signal was defined as the probability of firing synchronized spikes, and the noise was defined as the sum of spontaneous spikes and failures to spike in a given period. This procedure is illustrated in Figure 3C, to display the temporal precision and consistency of the evoked action potential signal, $S_{AP}(t)$, and its variance, $N_{AP}(t)$, by comparing several series of action potential responses to the pseudorandomly modulated displacement stimuli. Usually, there was remarkably little variance in action potential timing between different stimulus runs, so that the neurons produced reliable $S_{AP}(t)$ patterns with relatively small $N_{AP}(t)$.

Properties of the Signal and Noise Estimates

Figure 6 shows the signal and noise distributions of the receptor current and receptor potential data. Regardless of the mean displacement, both $N_{RC}(t)$ and $N_{RP}(t)$ distributions were Gaussian. The $S_{RP}(t)$ distribution was also Gaussian at high mean displacement (probably due to progressive activation of voltage-dependent potassium channels, whose shunting conductance would oppose large depolarizing transients), but $S_{RP}(t)$ at lower mean displacement and $S_{RC}(t)$ at both displacement levels were clearly skewed (cf. Juusola and French, 1995b, who showed that the skewness of $S_{RC}(t)$ results from the nonlinear transduction properties). Information capacities for both receptor potential and receptor current (Figure 3) were calculated at the higher mean displacement.

Signal Analysis in the Frequency Domain

For the two analog processes, the resulting signal and noise estimates were subjected to frequency domain analysis (see above). From each receptor current and receptor potential recording, we used an 8.192 s averaged response, i.e., the signal estimate, and 10–30 noise estimates of similar length. These were segmented for FFT-analysis using a Blackman-Harris four term window with 50% overlap of the segments (Bendat and Piersol, 1971; Harris, 1978). This gave 8 samples of signal spectra, $S_{xx}(f)_i$, and 80–240 samples of noise spectra, $N_{xx}(f)_i$, which were averaged in the frequency domain to give the receptor current and receptor potential signal, $S_{RC}(f)$ and $S_{RP}(f)$, and noise, $N_{RC}(f)$ and $N_{RP}(f)$, spectra, respectively. Finally, the signal-to-noise ratios of these two analog processes as functions of frequency, $SNR_{RC}(f)$ and $SNR_{RP}(f)$, were obtained from Equation 1. The action potential, $SNR_{AP}(f)$, was calculated from the corresponding coherence function, using Equation 2. Similar methods for defining the signal and noise have been used in fly photoreceptors (Juusola et al., 1994) and in the first graded potential synapse in the fly compound eye (Juusola et al., 1995; de Ruyter van Steveninck and Laughlin, 1996).

The averaged responses, i.e., receptor current, receptor potential, and action potential signals, now containing virtually no stimulus-independent noise, were segmented and used for FFT analysis, as explained above. Thereafter, the corresponding mechanoreceptor frequency responses, receptor current, $H_{RC}(f)$, receptor potential, $H_{RP}(f)$, and action potential, $H_{AP}(f)$, with their coherence function estimates $\gamma^2_{RC}(f)$, $\gamma^2_{RP}(f)$, and $\gamma^2(f)$, were calculated using the power spectra of the corresponding input (displacement stimulus, $D_{xx}(f)$) and output (mechanoreceptor signal, $S_{xx}(f)$) and their cross-power spectra ($S_xD_x(f)$; Bendat and Piersol, 1971; Marmarelis and Marmarelis, 1978). For example, in the case of action potentials, this was calculated from the cross correlation function between $S_{AP}(f)$ and the sample stimulus function $D_{xx}(f)$:

$$H_{xx}(f) = S_xD_x(f)/D_{xx}(f) \quad (4)$$

$$\gamma^2_{xx}(f) = [S_xD_x(f) \times S_xD_x(f)^*]/[D_{xx}(f) \times S_{xx}(f)] \quad (5)$$

where $S_xD_x(f)^*$ is the complex conjugate. Similarly, the membrane impedance, $H_{MI}(f)$ in Figure 2, was calculated by injecting pseudorandomly modulated current ($\pm$1 nA) and recording the resulting membrane potential at the same mean displacement level (5 $\pm$ 2 mm; cf. Juusola, 1994). The predicted receptor potential frequency response (i.e., first order approximation) was calculated by multiplying the membrane impedance, $H_{MI}(f)$, by the receptor current, $H_{RC}(f)$, both recorded at the same displacement level (5 $\pm$ 2 mm).

There are two advantages to using the previously defined $S_{AP}(t)$ values for estimating the frequency response function, $H_{AP}(f)$. First, the gain part is defined as the action potential probability evoked by the unit displacement modulation at each stimulus frequency. Second, it gives a direct estimate of the validity of the linear approximation for action potential encoding in the form of the coherence function. Based on our findings, linear system analysis is not sufficient to fully describe the action potential dynamics, but can still be used to approximate the neuronal performance.

Information Capacity during Action Potential Encoding

We used two different methods to estimate the information capacity of action potential encoding (mean ± SD). The first, based on linear assumptions, could be viewed as a lower limit of the estimate, whereas the second, based on maximum entropy, was free of linear assumptions.

Calculating directly from the coherence function between displacement and action potentials includes only the output that is linearly correlated with the input, and thus underestimates the actual information capacity. Combining Equation 2 and Equation 3:

$$R_{info} = \int \log_2[1/(1 - \gamma^2_{AP}(f))]df \quad (6)$$

gave the lowest value of 200 ± 40 bits/s (∼14% of the receptor current information).

For the maximum entropy method, the 1 ms bin size ensured that two spikes could not simultaneously occupy one bin. Thus, each bin contained either zero or one action potential. If action potentials occur at a rate R, the probability of finding an action potential in a bin was:

$$P = R^*\{\text{bin size}\} = R/1000 \quad (7)$$

Then, the entropy per bin was given by the expression:

$$E = -(P^*\log_2(P) + (1 - P)^*\log_2(1 - P)) \text{ bits} \quad (8)$$

During 8.192 s stimulation, the firing rates of different neurons varied from ∼40–90 action potentials/s, giving E = 0.24–0.44. The maximum entropy occurs when all bins are uncorrelated, in which case the total entropy is the sum of all of the single-bin entropies. In 1 s, there were 1000 bins, so the maximum spike train entropy rate varied from 240–440 bits/s. To get the information transmission rate, the equivocation must be subtracted from this. Only if the action potentials exactly repeat from trial to trial can the equivocation be zero and the information rate be the maximum entropy rate. The noise variance was 10–20% in different recordings, and consequently the information rates calculated in this way varied from 193–370 bits/s. These values were slightly higher than those derived from the coherence function.

Information Capacity with Arbitrary Noise

Limits for information capacity with arbitrary noise can be obtained if a finite bandwidth and limited average signal power are assumed. The limits are then given by:

$$W \log[(S + N_1)/N_1] \leq R_{info} \leq W \log[(S + N)/N_1] \quad (9)$$

where W is the bandwidth, S is the mean signal power, N is the mean noise power, and N_1 is the entropy power of the noise, obtained from:

$$N_1 = \exp[\int_w \log N(f) df/W] \quad (10)$$

where f is frequency and $N(f)$ is noise power, as before (Shannon and Weaver, 1949; Schwartz, 1963).

Acknowledgments

We thank M. Duszyk, M. J. Korenberg, H. P. C. Robinson, R. de Ruyter van Steveninck, E.-A. Seyfarth, G. Stroink, and C. Wall for critical reading of the manuscript, and three anonymous referees for interesting and constructive comments. This work was supported by the Medical Research Council of Canada, The Wihuri Foundation, and NATO.

Received January 7, 1997; revised May 1, 1997.

References

Barth, F.G. (1985). Slit sensilla and measurement of cuticular strains. In Neurobiology of Arachnids, F.G. Barth, ed. (Berlin: Springer-Verlag) pp. 163–188.

Barth, F.G., and Libera, W. (1970). Ein Atlas der Spaltsinnesorgane von Cupiennius salei Keys. Chelicerata (Araneae). Z. Morphol. Tiere. *68*, 343–369.

Bendat, J.S., and Piersol, A.G. (1971). Random Data, Analysis and Measurement Procedures. (New York: Wiley).

Bialek, W., Rieke, F., de Ruyter van Steveninck, R., and Warland, D. (1991). Reading a neural code. Science *252*, 1854–1857.

Bohnenberger, J. (1981). Matched transfer characteristics of single units in a compound slit sense organ. J. Comp. Physiol. [A] *142*, 391–402.

Chubbuck, J.G. (1966). Small-motion biological stimulator. APL Tech. Digest *5*, 18–23.

de Ruyter van Steveninck, R., and Laughlin, S.B. (1996). The rate of information transfer in graded-potential neurons and chemical synapses. Nature *379*, 642–645.

de Ruyter van Steveninck, R., and Bialek, W. (1988). Real-time performance of a movement-sensitive neuron in the blowfly visual system: coding and information transfer in short spike sequences. Proc. R. Soc. Lond. B *234*, 379–414.

French, A.S. (1992). Mechanotransduction. Annu. Rev. Physiol. *54*, 135–152.

French, A.S., and Holden, A.V. (1971). Alias-free sampling of neuronal spike trains. Kybernetik *8*, 165–171.

French, A.S., Holden, A.V., and Stein, R.B. (1972). The estimation of the frequency response function of a mechanoreceptor. Kybernetik *11*, 15–23.

Gabbiani, F., Metzner, W., Wessel, R., and Koch, R. (1996). From stimulus encoding to feature extraction in weakly electric fish. Nature *384*, 564–566.

Harris, F.J. (1978). On the use of the windows for harmonic analysis with the discrete Fourier transform. Proc. IEEE *66*, 51–84.

Juusola, M. (1994). Measuring complex admittance and receptor current by single electrode voltage clamp. J. Neurosci. Meth. *53*,1–6.

Juusola, M., and French, A.S. (1995a). Recording from cuticular mechanoreceptors during mechanical stimulation. Pflügers Arch. *431*,125–128.

Juusola, M., and French, A.S. (1995b). Transduction and adaptation in spider slit-sense organ mechanoreceptors. J. Neurophysiol. *74*, 2513–2523.

Juusola, M., Seyfarth, E.A., French, A.S. (1994). Sodium-dependent receptor current in a new mechanoreceptor preparation. J. Neurophysiol. *72*, 3026–3028.

Juusola, M., Uusitalo, R.O., and Weckström, M. (1995). Transfer of graded potentials at the photoreceptor–interneuron synapse. J. Gen. Physiol. *105*, 117–148.

Juusola, M., French, A.S., Uusitalo, R.O., and Weckström, M. (1996). Information processing by graded potential transmission through tonically active synapses. Trends Neurosci. *19*, 292–297.

Juusola, M., Seyfarth, E.A., and French, A.S. (1997). Fast coating of class-capillary microelectrodes for single-electrode voltage clamp in bath. J. Neurosci. Meth., in press.

Kouvalainen, E., Weckström, M., and Juusola, M. (1994). Determination of signal-to-noise ratio and linearity in light-adapted blowfly photoreceptors. Vis. Neurosci. *95*, 1221–1225.

Laughlin, S.B. (1987). Form and function in retinal processing. Trends Neurosci. *10*, 478–483.

Levin, J., and Miller, J. (1996). Broadband neural encoding in the cricket cercal sensory system enhanced by stochastic resonance. Nature *380*, 165–168.

Maier, R., and Seyfarth, E.-A. (1987). Heterogeneity of spider leg muscle: histochemistry and electrophysiology of identified fibres in the claw levator. J. Comp. Physiol. [B] *157*, 285–294.

Mainen, Z.F., and Sejnovski, T.J. (1995). Reliability of spike timing in neocortical neurons. Science *268*, 1503–1506.

Marmarelis, P.Z., and Marmarelis, V.Z. (1978). Analysis of Physiological Systems: The White Noise Approach (New York: Plenum).

Morris, C.E. (1990). Mechanosensitive ion channels. J. Membr. Biol. *113*, 93–117.

Robinson, H.P.C., and Kawai, N. (1993). Injection of digitally synthesized synaptic conductance transients to measure the integrative properties of neurons. J. Neurosci. Meth. *49*, 157–65.

Roddey, J.C., and Jacobs, G.A. (1996). Information theoretic analysis of dynamic encoding by filiform mechanoreceptors in the cricket cercal system. J. Neurophysiol. *75*, 1365–1376.

Sachs, F. (1986). Biophysics of mechanoreception. Membr. Biochem. *6*, 173–193.

Sakai, H.M., and Naka, K.-I. (1995). Response dynamics and receptive field organization of catfish ganglion cells. J. Gen. Physiol. *105*, 795–814.

Sakuranaga, M., Ando, Y.-I. and Naka, K.-I. (1987). Dynamics of the ganglion cell response in the catfish and frog retina. J. Gen. Physiol. *90*, 229–259.

Schwartz, L.S. (1963). Principles of coding, filtering, and information theory (Baltimore: Spartan Books Inc.).

Seyfarth, E.-A., and French, A.S. (1994). Intracellular characterization of identified sensory cells in a new mechanoreceptor preparation. J. Neurophysiol. *71*, 1422–1427.

Shannon, C.E. (1949). Communication in the presence of noise. Proc. IRE *37*, 10–21.

Shannon, C.E., and Weaver, W. (1949). The Mathematical Theory of Communication (Urbana: University of Illinois Press).

Stemmler, M. (1996). A single spike suffices: the simplest form of stochastic resonance in model neurons. Network: Computation in Neural Systems *7*, 687–716.

van Hateren, J.H. (1992). A theory of maximizing sensory information. Biol. Cybern. *68*, 23–29.

Wessel, R., Koch, C., and Gabbiani, F. (1996). Coding of time-varying electric field amplitude modulations in a wave-type electric fish. J. Neurophysiol. *75*, 2280–2293.